

Role of accidental torsion in seismic reliability assessment for steel buildings

Heui-Yung Chang¹, Chu-Chieh Jay Lin^{2*}, Ker-Chun Lin² and Jung-Yu Chen¹

¹*Department of Civil and Environmental Engineering, National University of Kaohsiung, No. 700, Kaohsiung University Rd., Kaohsiung, 81148, Taiwan*

²*National Center for Research on Earthquake Engineering, National Applied Research Laboratories, No.200 Sec.3, ShinHai Rd., Taipei, 10668, Taiwan*

(Received January 7, 2009, Accepted September 14, 2009)

Abstract. This study investigates the role of accidental torsion in seismic reliability assessment. The analyzed structures are regular 6-story and 20-story steel office buildings. The eccentricity in a floor plan was simulated by shifting the mass from the centroid by 5% of the dimension normal to earthquake shaking. The eccentricity along building heights was replicated by Latin hypercube sampling. The fragilities for immediate occupancy and life safety were evaluated using 0.7% and 2.5% inter-story drift limits. Two limit-state probabilities and the corresponding earthquake intensities were compared. The effect of ignoring accidental torsion and the use of code accidental eccentricity were also assessed. The results show that accidental torsion may influence differently the structural reliability and limit-state PGAs. In terms of structural reliability, significant differences in the probability of failure are obtained depending on whether accidental torsion is considered or not. In terms of limit-state PGAs, accidental torsion does not have a significant effect. In detail, ignoring accidental torsion leads to underestimates in low-rise buildings and at small drift limits. On the other hand, the use of code accidental eccentricity gives conservative estimates, especially in high-rise buildings at small drift limits.

Keywords : seismic performance; reliability-based assessment; fragility analysis; accidental torsion; mass eccentricity; steel buildings.

1. Introduction

Torsion vibration is an important cause of structural damage. Many factors, such as earthquake inelastic behavior and live load mass distribution, can cause the mass of a structure to deviate from the stiffness center. The discrepancy between mass center and stiffness center can lead a structure to undergo translation and torsion vibrations simultaneously, even though there is no base rotational excitation (Ayre 1938). To account for the induced torque, design codes have introduced an accidental eccentricity of 0.05 or 0.10 plan dimension parallel to the direction of eccentricity (e.g. Uniform Building Code (UBC) 1997, National Building Code of Canada (NBCC) 1995, Mexico City Building Code (MCBC) 1995, New Zealand Standard (NZS) 1992). A great deal of research has been made to evaluate the seismic performance of steel buildings and accidental torsion provisions (De la Llera and Chopra 1994a, 1994b, and 1994c, Huan and Liu 1994, Chandler and Duan 1997, Chandler, *et al.* 1997, Calderoni

* Corresponding Author, Email: jaylin@ncree.org

and Rinaldi 2002, Ozmen and Gulay 2002, Shakib and Tohid 2002, Jeng and Tsai 2002, Heredia-Zavoni and Leyva 2003, Stathopoulos and Anagnostopoulos 2003 and 2005, Vasilopoulos, *et al.* 2008)

By elastic response analyses, De la Llera and Chopra (1994a) investigated the accidental torsion effects arising from the discrepancies between the computed and actual values of structural element stiffness. They showed that the increase in structural deformations due to stiffness uncertainty is much smaller than implied by the accidental torsional provisions in the UBC and most other building codes. Huan and Liu (1994) studied the behavior of asymmetric buildings excited by incoherent seismic ground motions. They suggested that the accidental torsion effects arising from ground motion incoherence and structural irregularity could be approximated by a combination of the corresponding independent effects. De la Llera and Chopra (1994b) also analyzed the earthquake induced motions of three nominally symmetric-plan buildings. They found that base rotational motion can cause between 25% and 45% of the total accidental torsion in the buildings. De la Llera and Chopra (1994c) further estimated the increase in responses using actual base rotational excitations derived from ground motions recorded at the base of 30 buildings in California. They indicated that except for buildings with plan dimensions longer than 50 m, the computed accidental eccentricities are much smaller than the code values. In addition, the effect is more significant in symmetric buildings than in asymmetric buildings.

Shakib and Tohid (2002) used a three-dimensional single-story building model, evaluating the effect of earthquake rotational shaking on the accidental eccentricity of symmetric and asymmetric buildings. They confirmed De la Llera and Chopra's result (1994c) that the effect is more significant in symmetric buildings. They also showed that the effect of earthquake rotational shaking on the accidental eccentricity is more considerable on soft soils than on stiff soils. Heredia-Zavoni and Leyva (2003) drew a similar conclusion from the seismic torsion response of three-dimensional, multi-storey, multi-span symmetric, linear elastic buildings. The use of a code eccentricity to account for the accidental torsion due to ground spatial variations was assessed and it is concluded that the effect is overestimated on firm soils while underestimated on soft soils. However, incoherent and phase-delayed ground motions cannot induce a significant rotational response in a torsional stiff system which conflicts De la Llera and Chopra's estimation (1994c).

The above example not only reflects the difficulties in estimating the accidental torsion effects, but also suggests a necessity of re-examining the provisions using more real frame models. At the present stage, the accidental torsion effects cannot be fully simulated, and as a result are indeed generally not considered in the analysis. Chandler and Duan (1997) studied the performance of a single-storey torsional unbalanced model for serviceability and ultimate limit states. They indicated that including the code accidental eccentricity in determining the element strength could lead to an unsafe evaluation if the accidental torsion effects were ignored in the analysis. Stathopoulos and Anagnostopoulos (2003 and 2005) analyzed the inelastic torsion response of single-storey and multi-storey buildings using the shear-beam type models, and compared to that of more real frame models. They showed that there are great differences in the post-elastic eccentricities induced from non-symmetric yielding between frame buildings and simplified models.

The present study has performed a reliability-based seismic performance evaluation for a 6-story and 20-story regular steel office buildings. For buildings of regular configurations, the accidental torsion effects can arise from base rotational excitation and structural irregularity, such as an unfavorable distribution of live load mass and structural inelastic behavior (i.e. non-symmetric yielding (Stathopoulos and Anagnostopoulos 2003 and 2005)). The plan dimensions of the example buildings are not longer than 50 m, and the effect of base rotational excitation on the accidental eccentricity can be expected to be small (De la Llera and Chopra 1994b). The present study therefore only focuses on structural irregularity and the accidental torsion effects. The eccentricity in a floor plan is simulated by shifting the mass from

the centroid by 5% of the dimension normal to earthquake shaking. The eccentricity along building heights is also replicated by Latin hypercube sampling. The building responses are then estimated using three-dimensional nonlinear time history analysis. Attention has been given to the torsion arising from the distribution of live load mass. The effect of ignoring the accidental torsion and the use of code accidental eccentricity are also assessed. The results will help to gain a better understanding for the role of accidental torsion in seismic reliability assessment for regular buildings.

2. Performance evaluation

2.1 Example buildings

As shown by Fig. 1, the studied 6- and 20-story steel office buildings have the same floor plans (5×3 bays) with 9-m bay spacing while the height is 4.5 m at the first story and 4.0 m at the remaining floors (Wei 2006). The design dead load and live load are 6.5 kN/m^2 and 3.0 kN/m^2 , respectively. The masses of the floors are estimated using the dead load in addition to the live load of furniture and file cabinets, etc. All the beam-column connections are moment resisting. Load Resistance Factored Design (LRFD) has been adopted. Table 1 summarizes the member sizes and steel grades for the two buildings. The built-up box columns and H-shaped beams are also used in these buildings. The columns and beams are made of A572 Grade 50 steel ($F_y = 345 \text{ kPa}$) and A36 steel ($F_y = 248 \text{ kPa}$), respectively.

The buildings were designed for the peak ground acceleration (PGA) of 0.428 g (value from seismic hazard curve that has a 10% chance of exceedance in 50 years) in accordance with Taiwan's building code. In account of reparability performance and life-cycle financial success, the buildings were required to remain in elasticity when subjected to a small-to-moderate earthquake. This criterion controlled the structural design of the buildings. It was also confirmed that under design earthquake, the maximum drifts of the buildings might not exceed the 0.5% limit. An eigen-analysis was performed and the result showed that the fundamental periods of the 6-story and 20-story buildings are 1.48 sec and 3.10 sec, respectively. Besides, the two buildings sway in Z direction in the first mode of vibration.

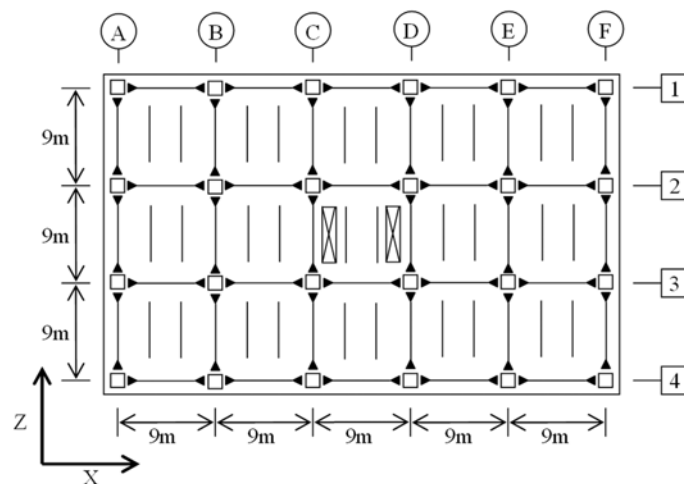


Fig. 1 Floor plan of 6- and 20-story buildings

Table 1 Member sizes and steel grades

(1) 6-story building (period for the 1st vibration mode = 1.48 sec)

Story	Column(A572)	Girder_X(A36)	Girder_Z(A36)
6F~5F	Box500 × 500 × 19	H488 × 300 × 11 × 18	H386 × 299 × 9 × 14
4F~3F	Box500 × 500 × 22	H494 × 302 × 13 × 21	H500 × 304 × 15 × 24
2F~1F	Box500 × 500 × 25	H588 × 300 × 12 × 20	H582 × 300 × 12 × 17

(2) 20-story building (period for the 1st vibration mode = 3.18 sec)

Story	Column(A572)	Girder_X(A36)	Girder_Z(A36)
20F~19F	Box500 × 500 × 19	H588 × 300 × 12 × 20	H582 × 300 × 12 × 17
18F~16F	Box600 × 600 × 28	H594 × 302 × 14 × 23	H594 × 302 × 14 × 23
15F~13F	Box700 × 700 × 25	H700 × 300 × 13 × 24	H700 × 300 × 13 × 24
12F~10F	Box700 × 700 × 28	H708 × 302 × 15 × 28	H708 × 302 × 15 × 28
9F~7F	Box750 × 750 × 25	H708 × 302 × 15 × 28	H712 × 306 × 19 × 30
6F~4F	Box750 × 750 × 28	H800 × 300 × 14 × 26	H800 × 300 × 14 × 26
3F~1F	Box750 × 750 × 32	H800 × 300 × 14 × 26	H800 × 300 × 14 × 26

2.2 Eccentricity cases

Codes often require incorporating accidental eccentricity in design. The uncertainties in earthquake rotational components, structural mass, stiffness, and strength, and an unfavorable distribution of live load mass are all considered. It is recommended to simulate the effect by moving the mass from the centroid by 5% of the plan dimension normal to earthquake shaking. In other words, all floors need to consider 5% mass eccentricity in design. On the other hand, most seismic evaluations have been made without accidental torsion effects.

Besides the above two cases, the present study considered another case for the torsion arising from the distribution of live load mass. In this case, the eccentricity in a floor plan was simulated by moving the mass from the centroid by 5% of the dimension normal to earthquake shaking. In addition, the eccentricity along building heights was replicated with the technique of Latin hypercube sampling (LHS) (McKay 1979, Iman, *et al.* 1981). In this way, arbitrary floors can have 5% mass eccentricity. Table 2 lists the sample points generated by LHS for the 6-story building.

It was assumed that there is 50% probability for a floor to have mass eccentricity. Following this presumption, the REC case will have a higher probability to occur and can be considered representative of what occurs in real buildings. Because the buildings sway in Z direction in the first mode of vibration, the shaking was assumed to be in Z direction. The floor mass was shifted along the x-axis passing the centroid by 5% of the plan length. The floor mass has the same probability to shift to the right or left of the centroid. The analysis adopted 8 different earthquake ground motions (see 3.1). Thus, the probability space was divided into 8 parts, and one eccentricity pattern was selected from each part. Each eccentricity pattern was finally assigned to one ground motion (see Table 2).

2.3 Response analyses

The building responses were simulated via a platform of inelastic structural analysis for 3D systems (Lin and Tsai 2006). The elastic-plastic behavior of columns and beams was replicated using plastic-

Table 2 Sample points generated by LHS for 6-story buildings ($\sqrt{}$ eccentricity)

Sample point	EQ.	2F		3F		4F		5F		6F		RF	
		Left	Right										
1	EQ4			$\sqrt{}$									
2	EQ6							$\sqrt{}$		$\sqrt{}$			
3	EQ2					$\sqrt{}$		$\sqrt{}$					$\sqrt{}$
4	EQ8		$\sqrt{}$		$\sqrt{}$					$\sqrt{}$		$\sqrt{}$	
5	EQ3		$\sqrt{}$	$\sqrt{}$		$\sqrt{}$		$\sqrt{}$				$\sqrt{}$	
6	EQ5					$\sqrt{}$		$\sqrt{}$			$\sqrt{}$		
7	EQ7		$\sqrt{}$	$\sqrt{}$			$\sqrt{}$		$\sqrt{}$	$\sqrt{}$		$\sqrt{}$	
8	EQ1	$\sqrt{}$			$\sqrt{}$								$\sqrt{}$

hinge models with bilinear stress-strain relations. In detail, the nominal yield strengths of A572 Grade 50 and A36 steels were used to estimate the flexural yield strength of columns and beams, respectively. In addition, the Young's modulus (200Mpa) and strain hardening ratio (0.05) obtained from experiments were used to predict the elastic and plastic stiffness. Furthermore, the LRFD interaction surface was used for considering the relations between axial forces and bending moments in columns.

A series of nonlinear time history analyses was carried out for the two example buildings. In brief, the earthquake shaking was assumed to be in Z direction. The masses of the floors were moved in the x-direction to replicate the code accidental eccentricity and the eccentricity patterns predicted by LHS (see the details in Table 2). The damping ratios for the first and second vibration modes were 2%. The results of the analyses confirmed that in moment resisting frames (MRFs), the inelastic behavior might be almost restricted to the plastic hinges in beams.

3. Fragility analyses

3.1 Ground motions

The randomness in earthquake excitations has been proven to be the main source of uncertainty (e.g. Wang and Foliente 2006). Numerous studies considered seismic input as the key random variable in the analysis (e.g. Song and Ellingwood 1999, Dymiotis, *et al.* 2001, Curadelli and Riera 2004, Wang and Foliente 2006, Li and Ellingwood 2007). To focus the effect of accidental torsion, the present study considers the seismic input in a similar way. As shown in Table 3, a set of 8 different acceleration time histories, corresponding to strong earthquake ground motions recorded in Asia and North America, was adopted (Curadelli and Riera 2004). As can be seen in Fig. 2, the earthquake ground motions have remarkable different characteristics. It can help to draw a general conclusion about the role of accidental torsion played in seismic reliability assessment.

The present study has performed a reliability-based seismic performance evaluation for a 6-story and 20-story regular steel office buildings. This kind of evaluation involves many issues about estimation accuracy and computation costs. The selection of earthquake ground motions with an appropriate earthquake ground motion intensity measure (*IM*) has played a key role in solving the issues. Previous work has shown that the same set of ground motions results in smaller conditional dispersion when the first mode spectral acceleration, denoted as S_a , is used as the *IM* rather than PGA (Luco and Cornell 2007).

Table 3 Ground motion records

	Earthquake site/component/data	Site conditions	Magnitude (M_w)	Distance (km)	PGA (g)
EQ1	Chi-Chi CHY010-E, Taiwan, Sep 21, 1999	Hard site	7.6	25.39	0.227
EQ2	Imperial Valley, El Centro 000, USA, Oct 15, 1979	Alluvium	6.5	8.3	0.349
EQ3	Kobe JMA NS, Japan, Jan 16, 1995	Shallow (stiff) soil	6.9	0.6	0.821
EQ4	Landers, Josuha Tree 000, USA, Jun 28, 1992	Deep narrow soil	7.3	11.6	0.274
EQ5	Llolleo 010, Chile, Mar 3, 1985	Sandstone, volcanic rock	7.9	34.1	0.712
EQ6	(6) Loma Prieta, Halls Valley, 000, USA, Oct 18, 1989	Deep narrow soil	6.9	31.6	0.134
EQ7	Northridge, Brentwood V.A. Hospital, 195, CA, USA, Jan 17, 1994	Deep broad soil	6.7	16.3	0.187
EQ8	San Fernando, Pasadena, Cit Athenaeum, 000, USA, Feb 9, 1971	Deep broad soil	6.6	31.7	0.088

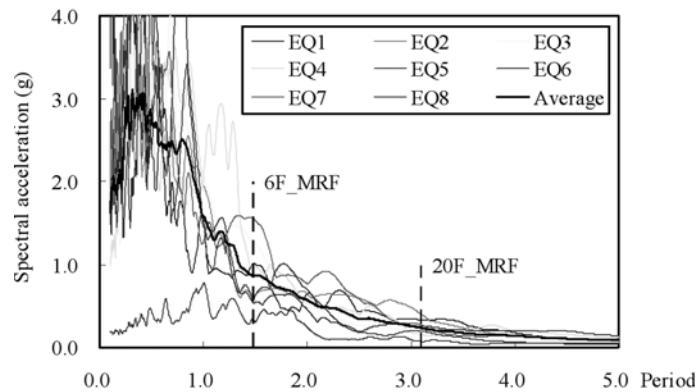


Fig. 2 Spectral acceleration (PGA = 1 g, damping ratio = 2%)

Nonetheless, it has also been demonstrated that S_a may not be particularly efficient nor sufficient for tall, long-period buildings as well as for near-source ground motions (Shome and Cornell 1999).

Compared to a scalar-valued IM such as S_a and PGA, a vector-valued IM has been proven to be more appropriate for the situation where a ground motion causes moderate to severe nonlinearity in a structural system (Backer 2007). However, modeling the interaction between IM parameters and estimating the seismic hazard still remains a challenge. Therefore, the adopted ground motions were normalized by their PGA, and then were scaled to increasingly higher intensity. As shown in Fig. 3, the same set of ground motions results in smaller conditional dispersion when PGA is used as the IM rather than S_a . In other words, PGA is relatively efficient in estimating the drift demands for the analyzed steel buildings of moderate-to-long period.

3.2 Failure Criteria

After obtaining the earthquake ground motion records, the fragility curve can be built by simulating

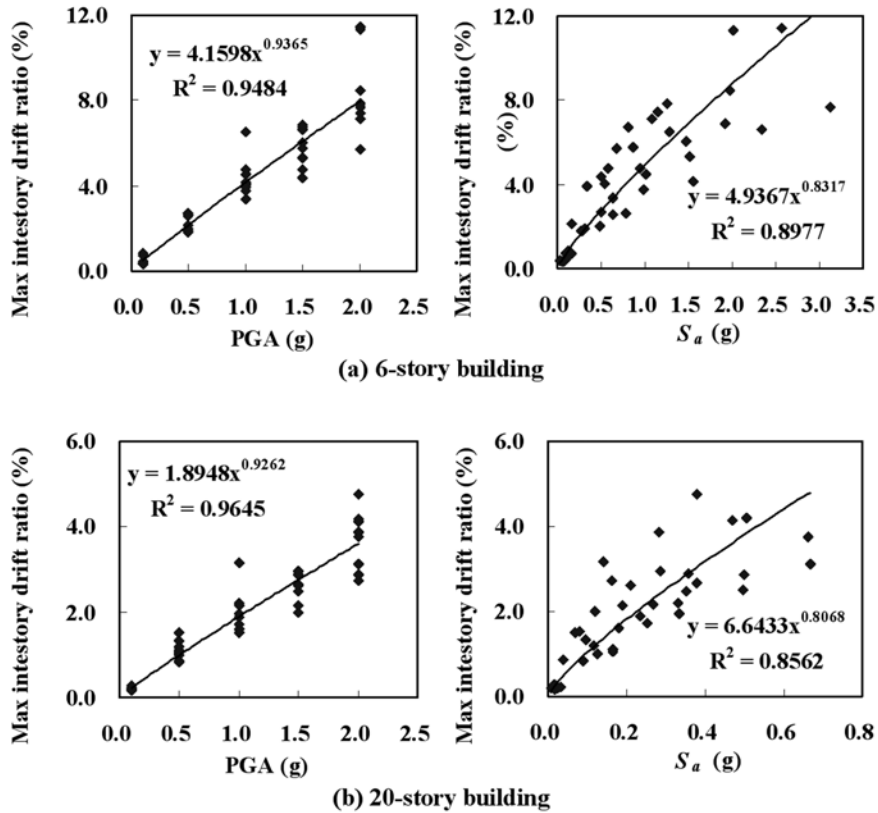


Fig. 3 Drift demands and earthquake intensity measures

and counting the relative number of failures for a specific limit state. The definition of a failure criterion to rigorously quantify the damage level of a structure is still an open question (Esteva, *et al.* 2001). However, post-earthquake disaster surveys have shown a correlation between excessive lateral drifts and damages for both structural and non-structural parts. This therefore study adapted the suggestions by FEMA 356, using 0.7% and 2.5% drift limits as the failure criteria for immediate occupancy and life-safety limit states.

When the studied fragilities are further applied to the fields of performance-based design and earthquake disaster prevention, the following two limit-state probabilities can be considered of great importance. One is the 10% failure probability for exceeding the limit state of immediate occupancy. The other is the 50% failure probability for exceeding the limit state of life safety. The former presents a state in which structural systems start to suffer non-structural damage and need repairs. The latter indicates a state in which the systems suffer severe structural damage and need further earthquake retrofitting. These two limit-state PGAs are selected for further comparison.

3.3 Fragility model

Before deriving the fragility curves, the seismic demands need to be related to the measure of earthquake intensity. In the present study, the relation between θ and PGA were approximated by the following equation,

$$\theta = a(PGA)^b \quad (1)$$

Where a and b are constants to be determined from a regression analysis.

The equation assumes that θ and PGA follow a lognormal distribution. Many studies have shown that the lognormal distribution can well fit the maximum structural response to earthquake ground motions at a specific exceedance probability level (e.g. Song and Ellingwood 1999). On the other hand, though the lognormal distribution predicts very high PGA with low probabilities, the estimate is still considered appropriate because the predicted PGA is within a few standard deviations of the median PGA (Holzer 2005).

The conditional probability that θ exceeds a defined drift limit ϕ , given a specific PGA, is

$$P_f(\theta > \phi | PGA = x) = 1 - \Phi(\ln|\phi/ax^b|/\beta_{\theta/PGA}) \quad (2)$$

In which $\Phi()$ is the standard normal distribution, and $\beta_{\theta/PGA}$ is a logarithmic standard deviation that can also be determined from a regression analysis. The above equations have provided a convenient way to predict the failure probability for exceeding stipulated drift limits and associated performance goals.

3.4 Capacity curves

In the present study, the maximum interstory drift ratio θ and PGA were taken as the main measures of seismic demands and earthquake intensity, respectively. The capacity curves of the 6-story buildings are depicted in Fig. 4. For the ease of discussion, the responses of torsion buildings are marked with “EC” and “REC”, in which, “EC” indicates buildings with code accidental eccentricity; while “REC” designates buildings with LHS eccentricity patterns (see the details in Table 2). To make a distinction, the responses of non-torsion buildings are marked with nothing.

As shown in Fig. 4, the buildings have similar responses at a PGA less than 1.0 g. The adopted 8 earthquake ground motions have very different spectral shapes (see Fig. 2). In addition, the buildings have many different eccentricity patterns (see Table 2). The result has suggested that eccentricity patterns and spectral shapes may have a small influence on drift responses to moderate shaking. As also can be seen in Fig. 4, when the PGA continues to increase, the responses vary significantly depending on eccentricity patterns and seismic waves. In other words, eccentricity patterns and spectral shapes may have a considerably large influence on drift responses to intensive shaking.

As shown in Fig. 2, EQ6 and EQ7 respectively cause the smallest and largest spectral acceleration at the fundamental period of the 6-story building. As illustrated by Table 2, the masses of the 5th and 6th floors were shifted to the right for EQ6 (i.e. sample point 2); whereas the masses of the 3rd and 6th floors were shifted to the left, and the masses of the other 4 floors were shifted to the right for EQ7 (i.e. sample point 7). As can be seen in Fig. 4, when the PGA achieves 1.5 g, the LHS eccentricity patterns (i.e. the REC cases) cause the largest and smallest responses to EQ6 and EQ7, respectively. When the PGA increases to 2 g, the LHS eccentricity patterns yield the smallest responses to EQ6 and EQ7.

Similar findings can also be obtained from the other examples of the 6-story buildings in Fig. 4. The examples have illustrated the difficulties and complexity in assessing accidental torsion, especially that arising from the distribution of live load mass. For the limit of space, the LHS eccentricity patterns and capacity curves of the 20-story buildings were not presented in this paper. The examples of the 20-story buildings also allowed making the same observation. The results help realize the importance and necessity of assessing the torsion effects on a reliability basis.

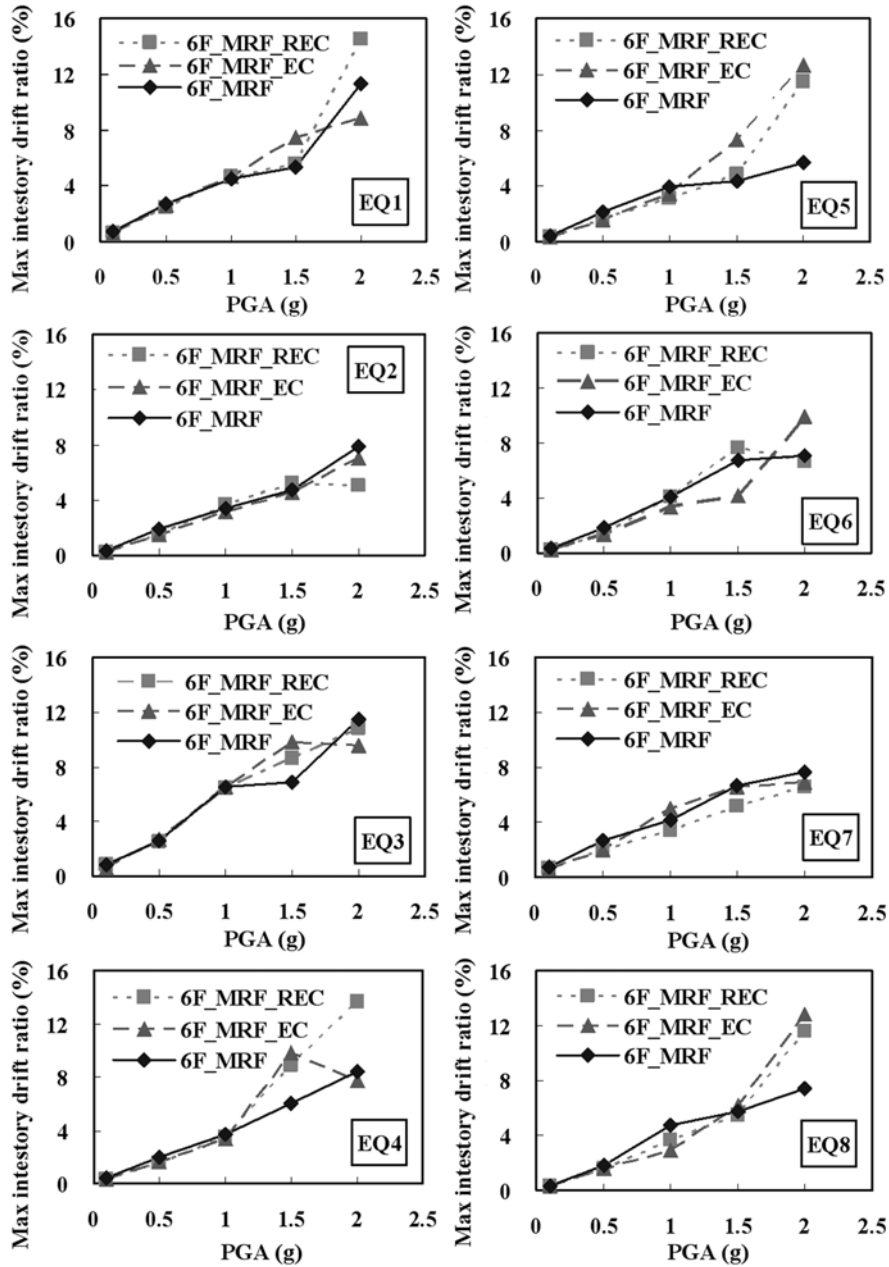


Fig. 4 Capacity curves of 6-story buildings

4. Results and discussion

4.1 Overall

The comparisons of the fragility curves for the 6- and 20-story buildings at 0.7% and 2.5% drift limit

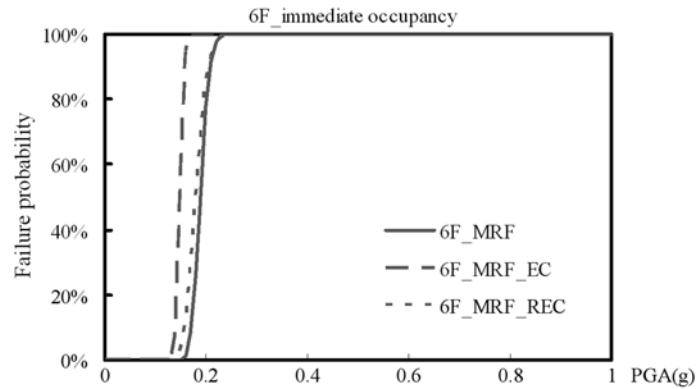


Fig. 5 Fragility curves for 6-story buildings at 0.7% drift limit

are shown in Figs. 5-8. In these figures, the fragility curves for torsion buildings are marked with “EC” and “REC”, in which, “EC” indicates buildings with 5% mass eccentricity at all floors that allows verifying the accidental torsion provisions while “REC” designates buildings with 5% mass eccentricity at arbitrary floors that enables to consider the torsion arising from the distribution of live load mass. To make a distinction, the fragility curves for non-torsion buildings are marked with nothing. That enables to assess the effect of ignoring accidental torsion.

Both the failure probabilities and limit-state PGAs can be used to assess the effects of accidental torsion. The two measures can cause different conclusions to be drawn from the same fragility curves. As mentioned in 3.2, two limit-state probabilities were considered of great importance. One was the 10% failure probability for exceeding the limit state of immediate occupancy. The other was the 50% failure probability for exceeding the limit state of life safety. The comparisons of the PGAs for the 6- and 20-story buildings to attain the two limit-state probabilities are shown in Tables 4 and 5. In these tables, the PGAs for the three eccentricity cases are normalized by the ones for the “REC” cases. The role of accidental torsion can therefore be investigated in a reasonable and efficient way.

4.2 6-story buildings

The fragility curves for the 6-story buildings at 0.7% drift limit are shown in Fig. 5. As can be seen, the fragility curve designated as “EC” always stays on the left side of the one marked with “REC”. It suggests that the code recommendation of 5% mass eccentricity at all floors may overestimate the fragilities for low-rise buildings. In the same figure, the fragility curve for the non-torsion building stays on the left side of the curves for the “REC” case. In addition, the two curves have a very small difference.

Table 4 Limit-state PGAs for 6-story buildings

6-story buildings		No mass eccentricity	Mass eccentricity at all floors	Mass eccentricity at arbitrary floors
$\theta \geq 0.7\%$	PGA (g)	0.171	0.140	0.157
$p_f = 10\%$	(Normalization)	(1.089)	(0.966)	(1.000)
$\theta \geq 2.5\%$	PGA (g)	0.625	0.585	0.620
$p_f = 50\%$	(Normalization)	(1.008)	(0.944)	(1.000)

It has implied that ignoring accidental torsion may underestimate the fragilities for low-rise buildings, but to a limited extent. The fragility curves for the 6-story buildings at 2.5% drift limit are depicted in Fig. 6. Comparing Figs. 5 and 6 enables to know that for low-rise buildings, accidental torsion may have similar effects on the fragilities for immediate occupancy and life safety. In detail, the code recommendation of 5% mass eccentricity at all floors overestimates the fragilities for life safety. In addition, ignoring accidental torsion causes an underestimate but considerably small difference.

The PGAs for the 6-story buildings to have 10% probability to exceed 0.7% drift limit and 50% probability to exceed 2.5% drift limit are summarized in Table 4. As can be seen in Table 4, the use of code accidental eccentricity (i.e. 5% eccentricity) decreases the limit-state PGAs by 3.4%-5.6%. On the other hand, ignoring accidental eccentricity (i.e. w/o eccentricity) increases the limit-state PGAs by 8.9%-0.8%. In brief, accidental torsion can only make a small difference to the limit-state PGAs for low-rise buildings.

4.3 20-story buildings

The fragility curves for the 20-story buildings at 0.7% drift limit are shown in Fig. 7. As can be seen,

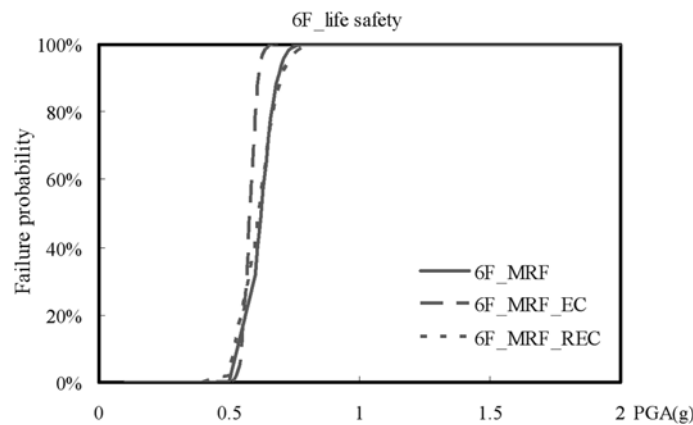


Fig. 6 Fragility curves for 6-story buildings at 2.5% drift limit

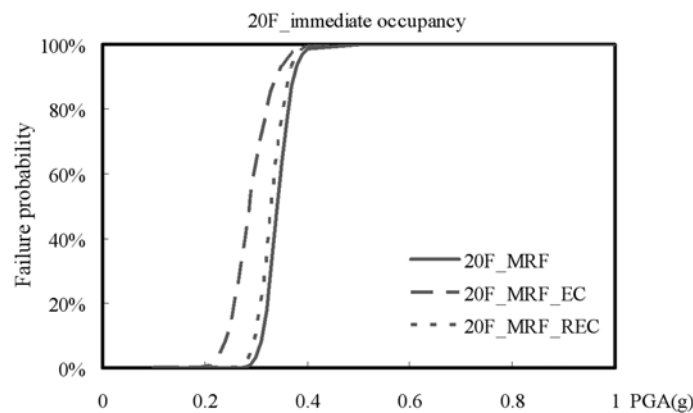


Fig. 7 Fragility curves for 20-story buildings at 0.7% drift limit

using the code accidental eccentricity (i.e. the “EC” case) leads to an overestimate. In contrast, ignoring accidental torsion gives a considerably small underestimate. Comparing Fig. 7 to Fig. 5 enables to know that for immediate occupancy or at a small drift limit, accidental torsion may have similar influence on the fragilities for high-rise and low-rise buildings. As illustrated by Fig. 5, the fragility curves for the 6-story buildings start to mount at PGAs less than 0.2 g. As also can be seen in Fig. 7, the fragility curves for the 20-story buildings start to raise at PGAs more than 0.2 g. In other words, the 20-story buildings can sustain shaking from a little stronger earthquake without any nonstructural damage. The result has implied that high-rise buildings are superior in reparability.

The fragility curves for the 20-story buildings at 2.5% drift limit are depicted in Fig. 8, in which, the fragility curves cross with each other. That means the use of code accidental eccentricity doesn’t always guarantee a conservative estimation. Similarly, ignoring accidental torsion doesn’t necessarily lead to an unsafe evaluation. Comparing Figs. 6 and 8 enables to know that for life safety or at a large drift limit, accidental torsion can have different influence on the fragilities for high-rise and low-rise buildings. As illustrated by Fig. 6, the fragility curves for the 6-story buildings start to mount at a PGA of 0.5 g. Also shown in Fig. 8, the fragility curves for the 20-story buildings start to rise at a PGA more than 1.0 g. In other words, the 20-story buildings can sustain stronger earthquake shaking without severe structural damage. The result of the above comparison agrees well with past experience that low-rise buildings are more vulnerable to seismic damage.

Table 5 summarizes the PGAs for the 20-story buildings to have 10% probability to exceed 0.7% drift limit and 50% probability to exceed 2.5% drift limit. As can be seen there, considering 5% mass eccentricity at all floors decreases the limit-state PGA by 18.5% at most. On the other hand, ignoring

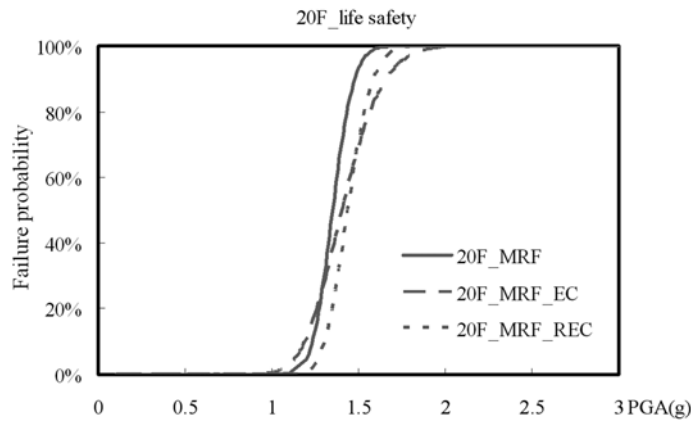


Fig. 8 Fragility curves for 20-story buildings at 2.5% drift limit

Table 5 Limit-state PGAs for 20-story buildings

20-story MRF		No mass eccentricity	Mass eccentricity at all floors	Mass eccentricity at arbitrary floors
$\theta \geq 0.7\%$	PGA (g)	0.310	0.243	0.298
$p_f = 10\%$	(Normalization)	(1.040)	(0.815)	(1.000)
$\theta \geq 2.5\%$	PGA (g)	1.343	1.393	1.429
$p_f = 50\%$	(Normalization)	(0.940)	(0.975)	(1.000)

accidental eccentricity causes the PGA to change 4.0%-6.0%. Thus, accidental torsion can only make a small difference to the limit-state PGAs for high-rise buildings. Comparing Tables 4 and 5 enables to know that the limit-state PGAs for the 20-story building are about twice large as those for the 6-story buildings. The result of the above comparison has implied that high-rise buildings may have greater resistance against strong earthquake shaking. It also suggests that ignoring accidental torsion can cause a larger underestimate in the fragilities for low-rise buildings at small drift limits. On the other hand, using the code accidental eccentricity may lead to a greater overestimate for high-rise buildings at small drift limits.

5. Conclusions

Codes often require incorporating accidental eccentricity in design. However, at the present stage the effects cannot be fully simulated, and are indeed generally not considered in the analysis. Previous studies have shown that the use of code accidental eccentricity can lead to an unsafe evaluation for the strength of structural member, if the effect is not included both in the design and analysis. On the other hand, simple models cannot replicate the non-symmetric yielding and post-elastic eccentricities in frame buildings. The present study therefore carried out a reliability-based seismic performance evaluation for 6- and 20-story regular steel office buildings. Detailed attention was given to the effects arising from an unfavorable distribution of live load mass and non-symmetric yielding in regular frame buildings. The effect of ignoring accidental torsion and the use of code accidental eccentricity were also assessed.

The fragility curves were derived for immediate occupancy and life safety using 0.7% and 2.5% drift limits. Two limit-state probabilities and the corresponding earthquake intensities were further compared. One was the 10% failure probability for exceeding the limit state of immediate occupancy while the other was the 50% failure probability for exceeding the limit state of life safety. The results show that accidental torsion may influence differently the limit-state PGAs and structural reliability. In terms of structural reliability, significant differences in the probability of failure are obtained depending on whether accidental torsion is considered or not. In terms of limit-state PGAs, accidental torsion does not have a significant effect. In detail, ignoring accidental torsion can lead to an unsafe evaluation for building fragilities and limit-state PGAs. It is especially true for low-rise buildings and at small drift limits. On the other hand, the use of code accidental eccentricity may give conservative estimates. Moreover, this trend will increase in high-rise buildings at small drift limits.

Acknowledgement

This study was partially supported by the National Science Council of the Republic of China under Grant No. NSC 98-2625-M-390-002, which is gratefully acknowledged.

References

- Ayre, R.S. (1938), "Interconnection of translational and torsion vibrations in buildings", *Seism. Soc. Am.*, **28**(2), 89-130.
- Backer, J.W. (2007), "Probabilistic structural response assessment using vector-valued intensity measures",

- Earthq. Eng. Struct. D.*, **36**(5), 1861-1883.
- Calderoni, B. and Rinaldi, Z. (2002), "Seismic performance evaluation for steel MRF: nonlinear dynamic and static analyses", *Steel Compos. Struct.*, **2**(2), 113-128.
- Chandler, A.M., Correnza, J.C. and Hutchinson, G.L. (1997), "Inelastic response of code-designed eccentric structures subject to bi-directional loading", *Struct. Eng. Mech.*, **5**(1), 51-58.
- Chandler, A.M. and Duan, X.N. (1997), "Performance of asymmetric code-designed buildings for serviceability and ultimate limit states", *Earthq. Eng. Struct. D.*, **26**(7), 717-735.
- Curadelli, R.O. and Riera, J. D. (2004), "Reliability based assessment of metallic dampers in buildings under seismic excitations", *Eng. Struct.*, **26**, 1931-1938.
- De la Llera, J.C. and Chopra, A.K. (1994), "Accidental torsion in building due to base rotational excitation", *Earthq. Eng. Struct. D.*, **23**(9), 1003-1021.
- De la Llera, J.C. and Chopra, A.K. (1994), "Accidental torsion in building due to stiffness uncertainty", *Earthq. Eng. Struct. D.*, **23**(2), 117-136.
- De la Llera, J.C. and Chopra, A.K. (1994), "Evaluation of code accidental-torsion provisions from building records", *J. Struct. Eng.*, **121**(2), 597-616.
- Dymiotis, C., Kappos, A.J. and Chryssanthopoulos, M.K. (2001), "Seismic reliability of masonry-infilled RC frames", *J. Struct. Eng.*, **127**(3), 296-305.
- Esteva, L., Daz-Lpez, O. and Garca-Prez, J. (2001), "Reliability functions for earthquake resistant design", *Reliab. Eng. Syst. Safe.*, **73**, 239-262.
- FEMA 356 (2000), *Prestandard and Commentary for the Seismic Rehabilitation of Buildings*, Federal Emergency Management Agency, Washington, D.C.
- Heredia-Zavoni, E. and Leyva, A. (2003), "Torsional response of symmetric buildings to incoherent and phasedelayed earthquake ground motion", *Earthq. Eng. Struct. D.*, **32**(7), 1021-1038.
- Holzer, T.L. (2005), "Comment on comparison between probabilistic seismic hazard analysis and flood frequency analysis", *Eos Trans.*, **86**(33), 305.
- Huan, G.D. and Liu, X. (1994), "Torsion response of unsymmetric buildings to incoherent ground motions", *J. Struct. Eng.*, **120**(4), 1158-1181.
- Iman, R.L., Helton, J.C. and Campbell, J.E. (1981), "An approach to sensitivity analysis of computer models, Part 1. Introduction, input variable selection and preliminary variable assessment", *J. Qual. Technol.*, **13**(3), 174-183.
- Jeng, V. and Tsai, Y.L. (2002), "Correlation between torsional vibration and translational vibration", *Struct. Eng. Mech.*, **13**(6), 671-694.
- Li, Y. and Ellingwood, B.R. (2007), "Reliability of woodframe residential construction subject to earthquakes", *Struct. Saf.*, **29**, 294-307.
- Lin, B.Z. and Tsai, K.C. (2006), *Platform of inelastic structural analysis for 3D systems - PISA3D R2.0.2 users manual*, National Center for Res. on Earth. Eng.
- Luco, N. and Cornell, C.A. (2007), "Structure-specific scalar intensity measures for near-source and ordinary earthquake ground motions", *Earthq. Spectra.*, **23**(2), 357-392.
- McKay, M.D., Conover, W.J. and Beckman, R.J. (1979), "A comparison of three methods for selecting values of input variables in the analysis of output from a computer code", *Technometrics*, **21**, 239-245.
- Mexico City Building Code (MCBC) (1995), *Mexico City Building Code, Complementary Technical Norms for Earthquake Resistant Design*, Dept. del Distrito Federal, Mexico, DF, Mexico.
- National Building Code of Canada (NBCC) (1995), *Associate Committee on the National Building Code*, National Council of Canada, Qubee, Canada.
- New Zealand Standard (NZS) (1992), *4203:1992, General Structural Design and Design Loadings for Buildings*, Standards Assoc. of New Zealand, Wellington New Zealand.
- Ozmen, G. and Gulay, F.G. (2002), "An investigation of torsionally irregular multi-story buildings under earthquake loading", *Struct. Eng. Mech.*, **14**(2), 237-243.
- Shakib, H. and Tohid, R.Z. (2002), "Evaluation of accidental eccentricity in buildings due to rotational component of earthquake", *J. Earth. Eng.*, **6**(4), 431-445.
- Shome, N. and Cornell, C.A. (1999), *Probabilistic seismic demand analysis of nonlinear structures*, RMS-35, RMS Program, Stanford (CA), 320p < <http://www.stanford.edu/group/rms/> >.

- Song, J. and Ellingwood, B.R. (1999), "Seismic reliability of special moment steel frames with welded connections: I and II", *J. Struct. Eng.*, **125**(4), 357-384.
- Stathopoulos, K.G. and Anagnostopoulos, S.A. (2003), "Inelastic earthquake response of single-story asymmetric buildings: an assessment of simplified shear-beam models", *Earthq. Eng. Struct. D.*, **32**(12), 1813-1831.
- Stathopoulos, K.G. and Anagnostopoulos, S.A. (2005), "Inelastic torsion of multi-storey buildings under earthquake excitations", *Earthq. Eng. Struct. D.*, **34**(12), 1449-1465.
- Uniform Building Code (UBC) (1997), *Int. Conf. of Building Officials*, Whittier, California.
- Vasilopoulos, A.A., Bazeos, N. and Beskos, D.E. (2008), "Seismic design of irregular space steel frames using advanced methods of analysis", *Steel Compos. Struct.*, **8**(1), 53-83.
- Wang, C.H. and Foliente, G.C. (2006), "Seismic reliability of low-rise nonsymmetric woodframe buildings", *J. Struct. Eng.*, **132**(5), 733-744.
- Wei, C.Y. (2006), "A study of local buckling BRB and cost performance of BRBF", Thesis for the M.S. degree at National Taiwan Univ.